7. Xiang-Yang Wang, Yang-Cheng Liu, Hong-Ying Yang. Image denoising in extended Shearlet domain using hidden Markov tree models. Digital Signal Processing, 2014, pp. 30-41.
8. Hong-Ying Yang, Xiang-Yang Wang, Pan-Pan Niu, Yang-Cheng Liu. Image denoising using non subsampled shearlet transform and twin support vector machines. Neural Networks, 2014, pp. 57-69.

Research on High Frequency Dynamic Bridge Deflection Detection Based on Digital Imaging

Yude Xiao*[1], Shaowen Sun[2], Qiang Guo[3], Guoxi Tang[4]

1.Anhui Communications Vocational &Technical College, 230051, Hefei, China*
2. Anhui Water Resources Department, 230022, Hefei, China
3. Anhui Communications Vocational &Technical College, 230051, Hefei, China
4. Anhui Transport Consulting & Design Institute Co., Ltd, 230088, Hefei, China

Abstract
This paper presents a measurement method of dynamic bridge deflection detection in high frequency based on digital imaging technology. This system based on digital imaging theory and the hardware including matrix camera, long telephoto lens, laser rangefinder, target markers, auxiliary lighting, and industrial tablet. Target markers were continuously collected by the camera in high frequency, wirelessly transferred to industrial tablet. Based on the algorithm of HALCON, target images were recognized by user application program which is developed under Visual Studio 2010 C++. By calculating the center position of the target image, the target markers displacement is achieved. Experiments show that the method can achieve the detection accuracy of 0.1 mm and this method is characterized with non-contact, remote and dynamic automated detection, high precision, etc.
Keywords: DEFLECTION, BRIDGE, IMAGING, CAMERA, DYNAMIC

1. Introduction

Deflection is a very important indicator in bridge security evaluation, which directly reflects the carrying capacity of the bridge structure. The value of bridge deflection needs to be measured accurately in both static and dynamic state in bridge test, as well as unsafe bridge renovation and new bridge acceptance. The impact coefficient and structural internal force distribution of loads can be drawn from numerical analysis of dynamic deflection to determine the integrity of the weak parts of bridges [1]. Traditional bridge deflection detecting methods are as follows: dial indicator, level gauge and theodolite. Modern measurement ways include line CCD, total station instrument, communication pipe, inclinometers, laser imaging, and differential GPS [2-4].

Digital image processing technology has developed rapidly in recent years [5-6]. In 1997, Hans-Gerd.Maas used a digital camera Kodak DSC460 to monitor the Switzerland Nalps dam [7]. Experimental results showed that the accuracy of the method have reached 1.8~3.7mm (about 1/15 pixel) in all directions. In 2001, Sangho from South Korea developed a software system [8], which employed close-range photogrammetry techniques for structural displacement analysis. He built a suspension bridge model experiment by using Kodak DSC200, Samsung SV-D100 and Nikon F-801. The experiment focused on the image segmentation algorithm and positioning accuracy, and point out that to promote the application in engineering further improvement of measurement accuracy and real-time online monitoring should be achieved. In 2002, T.White used JAI-M50 1/2 CCD camera and LVDT measuring the vertical displacement of concrete beam [9]. The results showed that photography can achieve sub-micron degree, consistent with the results measured by LVDT. In 2006, Hans-Gerd.Maas obtained a more satisfactory result in material tests, using high-speed cameras measuring material deformation values [10]. Ruinian Jianget developed a measuring system to test a bridge structure which based on the principle of close-range photogrammetry in 2010 [11]. The accuracy of this system achieved 1mm which is better than the traditional measurement. Zeynep in 2011 measured the displacement of same position in a bridge with two independent methods: photogrammetry and displacement sensors [12]. The results agree with each other in comparison.

2. Overview of the System

2.1. Hardware

The hardware of the system is composed of industrial tablet PC produced by Panasonic, Canon 6D SLR (body), Celestron NexStar8 SE telescope, Leica D8 laser rangefinder, target marker, and manipulating console of the telescope. The target marker is joint with bridge solidly and supposed to be mounted on the point where has the max deformation. As the bridge loaded and distort, the target marker can move with bridge. Based on MFC, our bridge deflection detecting software can run on the PC. Shooting parameters of Canon 6D can be set by the soft. Adjust the focal length to get a clear imaging. Under 1280*720 resolution, the camera can reach a frame rate as high as 60fps. The pictures transmitted to IPPC through WLAN. The laser rangefinder installed on the side of the lens to measure the distance between target marker and the optical center. Bluetooth 2.0 is used to control the laser rangefinder as well as data transmission. Here is the structure of the hardware system shows in Figure 1.

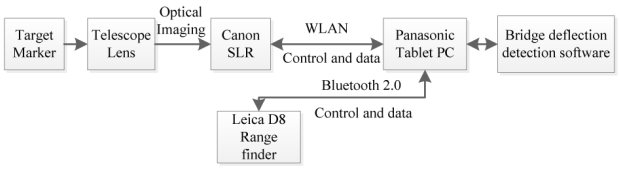

Figure 1. Hardware System

2.2. Software

Based on the Platform of Visual Studio 2010, the bridge deflection detecting software is designed with MFC. The software mainly includes pictures and data gathering module, deflection detecting module and camera calibration module. Structure of the software is shown in Figure 2.

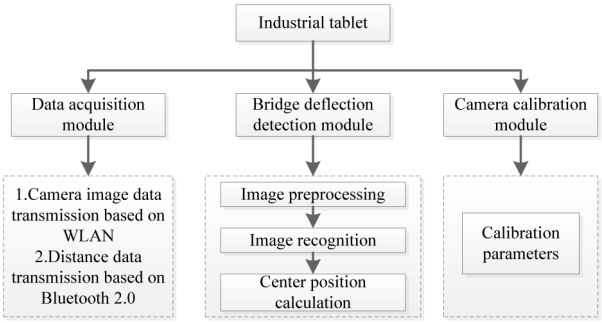

Figure 2. Software System

3. Detection principle

As shown in Figure 3, the target marker is mounted on a bridge with a rigid connection. When the bridge is under load, the bridge will produce a ΔH deformation. The target center will also have the corresponding ΔH displacement. Through the optical system, the target image on the CMOS sensor also produced a Δh corresponding displacement. The mathematical relationship between ΔH and Δh follow pinhole imaging principle. If the physical size of a single pixel on the CMOS sensor is p. While the image analysis software calculates the moving pixels of the center point for the n. Then there is $\Delta H = n \times p$. Figure 4 shows the relationship between camera coordinates (X_C, Y_C, Z_C), pixel coordinates (u, v), and image plane coordinates (x, y). According to the projection relationship, here are the following equations (1) and (2):

$$\begin{bmatrix} u \\ v \\ 1 \end{bmatrix} = \begin{bmatrix} 1/dx & 0 & u_0 \\ 0 & 1/dy & v_0 \\ 0 & 0 & 1 \end{bmatrix} \quad (1)$$

$$Z_C \begin{bmatrix} x \\ y \\ 1 \end{bmatrix} = \begin{bmatrix} f & 0 & 0 \\ 0 & f & 0 \\ 0 & 0 & 1 \end{bmatrix} \bullet \begin{bmatrix} X_C \\ Y_C \\ Z_C \end{bmatrix} \quad (2)$$

So there are equations (3) and (4):

$$X_C = \frac{(u-u_0)\times Z_C \times dx}{f} \quad (3)$$

$$Y_C = \frac{(v-v_0)\times Z_C \times dy}{f} \quad (4)$$

At a certain distance, from camera optical system we can see that the focal length is constant. The (u_0, v_0) stands for the number of pixels on the camera optical center to pixel coordinate origin which is also constant. Z_C is the distance measured by the laser range finder. dx and dy mean each pixel element corresponding to the physical dimensions of the X direction and Y direction. So, we can get the equation (5) as follow:

$$Y_C = (Av + B)\times Z_C \quad (5)$$

In order to correct the errors caused by other factors, the two polynomials Av^2 are introduced here in equation (6).

$$Y_C = (Av^2 + Bv + C)\times Z_C + D \quad (6)$$

In the equation (6), A, B, C and D are the parameters to be calibrated.

4. Identification and Calculation of Target Maker

Automatic target recognition and center position calculation are important to the accuracy of deflection detection. The target marker is shown in Figure (5). The size of the target marker is 180mm*180mm. The outer ring is a square and contains four circles which are 30.000 mm in diameter. Between the two circles distance is 60.000 mm. The upper left corner is designed with a 45 degree mark. This target can satisfy the detection distance from 15m to 60m. For a further distance, the marker can be designed for different sizes.

Our goal is to obtain the coordinates of the center of the four circle of ABCD, then calculate the mean value equation (7). So the target center point coordinate is:

$$v = \sum_{i=1}^{4} v_i \Big/ 4 \quad (7)$$

It mainly includes three parts: image pre-processing, target recognition and center coordinate calculation. The main steps of image pre-processing are as follows: big template average filtering, image difference, small template average filtering, dynamic threshold segmentation, region connection, ROI (Region of Interesting) selection based on the shape, binarization image.

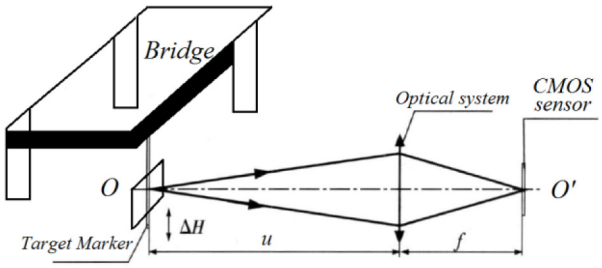

Figure 3. Camera Detection Principle

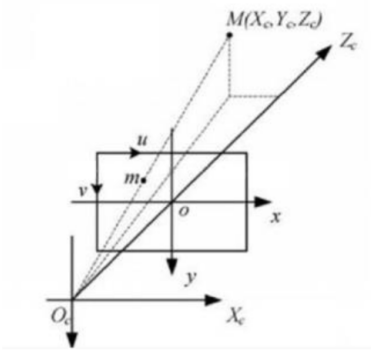

Figure 4. The Relationship between the Three Coordinates

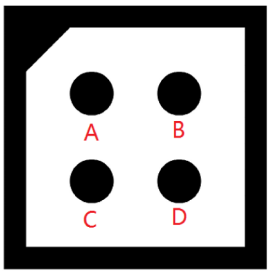

Figure 5. The Target Marker

The identification of target marker mainly uses the HALCON operators 'find_caltab' and 'find_marks_and_pose'. The 'find_caltab' operator includes six variables: the input image, the output image, calibration target description file, gauss filter size, the minimum threshold, the maximum threshold. The processing procedure of the operator is: firstly, take Gauss filtering on the input image then do the threshold segmentation, and template matching based on the calibration description file, search calibration target area. The operator 'find_marks_and_pose' has thirteen variables, they are: image input, calibration region image output, calibration board description files, camera internal parameters, initial gray of edge detecting, step length, and minimum gray of edge detection, coefficient of edge detection filter, minimum contour length, mark maximum diameter, the array of

marking point row coordinate, the array of marking point column coordinate, the estimated camera external parameters. The processing procedure of operator is: using the calibrating board area which operator find_caltab calculated to do the edge detection, calculating the circles' diameter, perimeter and the coordinate of the circle center position of dots, and comparing with calibration board description file, output the center coordinates of each dots. The automatic target recognition process is shown in Figure (6)

Part of the key code is shown in Figure (7):

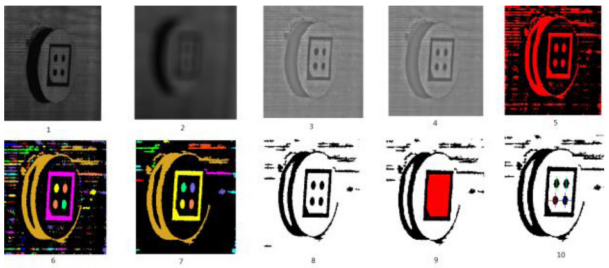

Figure 6. The Process of Automatic Target Recognition

```
CamPara:= [2.032, 0, 6.47e-006, 6.47e-006, Column/2, Row/2, Column, Ro
w]
find_caltab(ImageResult, PlateRegion, 'C:/caltab/caltab-180.descr', 3,
128, 5)
find_marks_and_pose (PlateRegion, PlateMarks, 'C:/caltab/caltab-180.de
scr', CamPara, 255, 5, 1, 0.6, 20, 60, RCoord, CCoord, StartPose)
```

Figure 7. Part of the key code

5. Calibration and Experiment

Using the calibration principle of the previous description, we carried out the calibration experiments at a distance of 45.438 meters. Move the calibration plate in the vertical direction from the base position up and down to 1 mm and the step size of each moving is 0.1 mm. The deflection detection software collects the images after each move. Then calculate the change pixel values of the center point in the calibration plate image. We use the Marquardt method and general global optimization method to calculate the value of the coefficient in the equation (6). Table 1 is the coefficient. Table 2 is a comparison between calculated value by the software and true measured value after the calibration.

Table 1. The calibrated coefficient

A	1.124917E-6
B	0.003572
C	-691.836608
D	31435.667714

Table 2. The Result of Calculated and the Measured Values.

Measured Value(mm)	Calculated value(mm)	Difference(mm)
-1	-0.99383	-0.00617
-0.9	-0.91136	0.011363
-0.8	-0.80783	0.007833
-0.7	-0.70912	0.009118
-0.6	-0.59417	-0.00583
-0.5	-0.51319	0.013193
-0.4	-0.4014	0.001401
-0.3	-0.30739	0.007392
-0.2	-0.20686	0.006863
-0.1	-0.10143	0.001426
0	0.004053	-0.00405
0.1	0.096586	0.003414
0.2	0.197274	0.002727
0.3	0.298	0.002
0.4	0.405269	-0.00527
0.5	0.512582	-0.01258
0.6	0.616686	-0.01669
0.7	0.717576	-0.01758
0.8	0.80548	-0.00548
0.9	0.911331	-0.01133
1	1.020483	-0.02048

Figure (8) shows the actual measurement curve which is completed in an experiment of the bridge deflection detection. We set the experiment on a bridge which is under construction. Bridge span is 100 meters, and the target marker is placed in the middle of the bridge. In the detection software, there are camera parameters setting, camera calibration, graphics, image acquisition real-time display, detection window display, data storage and other functions.

Figure (9) is the installation position of the target marker in our test bridge. The detection device is shown in Figure (10).

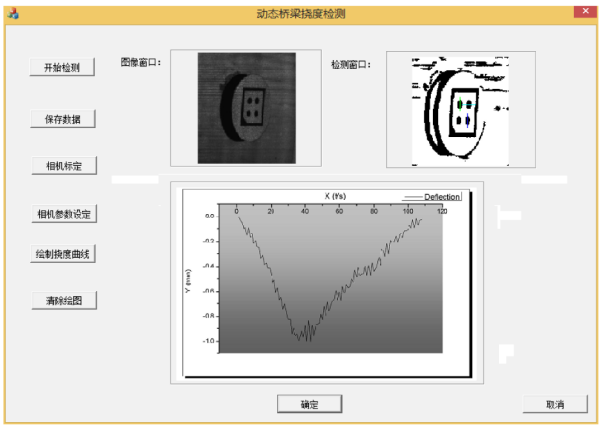

Figure 8. Detection Software

Figure 9. The Position of Target Marker in Test Bridge

Figure 10. The Detection Device

Conclusions

This paper is based on the principle of digital imaging. Focus on high frequency dynamic detection of bridge deflection. We have built a bridge deflection detection system and written an application of deflection detection based on the MFC. Through the experiment, we verify the feasibility and accuracy of the system. Experiment shows that this method can detect the deflection of the bridge in real time and can achieve the detection accuracy of 0.1mm. Compared with the traditional bridge deflection detection, the system has many advantages, such as simple structure, high accuracy, real time and so on. We can replicate this system and set multiple targets marker on the bridge to realize multi point synchronous detection. So, we can achieve the bridge deflection curve drawing and data extraction for bridge construction and maintenance work.

References

1. Zhang Shan, Research of XXXX, Proceedings of Conference"ICEIC – 2007", Beijing, 2008, pp. 245-248.
2. BIAN Yu-sheng. Discussion on a New Measurement Way for Bridge Deflection. Journal of Railway Engineering Society, 2008, 07, pp.53-56.
3. Wang Hongwei, Zhao Guoqing, Tan Heng. Application of linear CCD in bridge vibration non-contact measurement. Electronic Measurement Technology, 2007, 08, pp.65-67.
4. ZENG wei, YU De-jie, etc. An Auto-Monitoring System Based on the Communicating Pipe Principle of Bridge Deflection. Journal of Hunan University (Natural Sciences), 2007, 07, pp.44-47.
5. Yan Yu, Haoyuan Xie, Jie Wang. Deflection measurement using wireless inclination sensors for bridge. Intelligent Control and Information Processing, Dalian, 2010, pp.487-492.
6. Jong Jae Lee, Masanobu Shinozuka. A vision-based system for remote sensing of bridge displacement. NDT & E International, 2006, July, Vol39, 5, pp.425-431.
7. Ming Yang, Weiguo Di, Yuebo Wang. Bridge Monitoring System Based on Distribution Network Sensor, Automation and Logistics, Jinan, 2007, 18-21, Aug, pp.1524-1527.
8. Hans-Gred Maas. Photogrammetric Techniques for Deformation Measurements on Reservoir Wall. LAG SC4 Symposium Geodesy for Geotechnical and Structural. Engineering Eisenstadt.1998, pp.20-22.
9. Sangho B. The Component Development of Digital Close Range Photogrammetry for the Construction Structure Displacement Analysis. New Technology for a New Century International Conference, Seoul, Korea, pp.2001.6-11.
10. T. White man, D .D, Lichti I, Chandler. Measurement of deflection in concrete beams by close-range digital photogrammetry. Symposium on Geospatial theory, 2002, pp.9-12.
11. Hans-Gred maas, Uwe Hampel, Photogrammetric Techniques in Civil Engineering Material. Testing and Structure Monitoring, 2007, pp.39-45.
12. Ruinian Jiang, David v. Jauregui. Development of a Digital Close-range Photogrammetric Bridge deflection Measurement System. Measurement, 2010, pp.1431-1438.
13. Zeynep Firat Alemdar, JoAnn Browning etc. Photogrammetric measurement of RC Bridge Column deformations. Engineering Structures, 2011, pp.2407-2415.